The *Drosophila* F-box protein dSkp2 regulates cell proliferation by targeting Dacapo for degradation

Wen Dui[a,b,c], Bin Wei[a,b], Feng He[c], Wei Lu[a], Changqing Li[a], Xuehong Liang[a], Jun Ma[a,c,d,e], and Renjie Jiao[a,e]

[a]State Key Laboratory of Brain and Cognitive Science, Institute of Biophysics, Chinese Academy of Sciences, Beijing 100101, China; [b]University of Chinese Academy of Sciences, Beijing 100080, China; [c]Division of Biomedical Informatics and [d]Division of Developmental Biology, Cincinnati Children's Research Foundation, Cincinnati, OH 45229; [e]Department of Chemistry and Biology, National University of Defense Technology, Changsha 410072, China

ABSTRACT Cell cycle progression is controlled by a complex regulatory network consisting of interacting positive and negative factors. In humans, the positive regulator Skp2, an F-box protein, has been a subject of intense investigation in part because of its oncogenic activity. By contrast, the molecular and developmental functions of its *Drosophila* homologue, dSkp2, are poorly understood. Here we investigate the role of dSkp2 by focusing on its functional relationship with Dacapo (Dap), the *Drosophila* homologue of the cyclin-dependent kinase inhibitors p21^{cip1}/p27^{kip1}/p57^{kip2}. We show that dSkp2 interacts physically with Dap and has a role in targeting Dap for ubiquitination and proteasome-mediated degradation. We present evidence that dSkp2 regulates cell cycle progression by antagonizing Dap in vivo. *dSkp2* knockdown reduces cell density in the wing by prolonging the cell doubling time. In addition, the wing phenotype caused by *dSkp2* knockdown resembles that caused by *dap* overexpression and can be partially suppressed by reducing the gene dose of *dap*. Our study thus documents a conserved functional relationship between dSkp2 and Dap in their control of cell cycle progression, suggesting the possibility of using *Drosophila* as a model system to study Skp2-mediated tumorigenesis.

INTRODUCTION

In eukaryotes, cell cycle progression requires the activation of a series of cyclin-dependent protein kinases (CDKs) in combination with their partner cyclins at specific points (Morgan, 1995). For example, progression through the G1 restriction point in animal cells is controlled by the Cdk4/CycD and Cdk6/CycD complexes, and the transition from G1 to S phase is achieved through the Cdk2/CycE complex (Vermeulen *et al.*, 2003). CDK inhibitors (CKIs) are negative regulators of cell cycle progression by inhibiting the activity of CDK–cyclin complexes. Members of the Cip/Kip family of CKIs inhibit the G1 to S transition by associating with, and inhibiting the activity of, the Cdk2/CycE complex (Wojda, 2000).

In humans, there are three Cip/Kip family members: p21^{cip1}, p27^{kip1}, and p57^{kip2}. The activities of these proteins are subject to negative regulation by SCF^{Skp2} (Yu *et al.*, 1998; Amati and Vlach, 1999; Carrano *et al.*, 1999; Tsvetkov *et al.*, 1999; Kossatz *et al.*, 2004; Nakayama *et al.*, 2004; Pagano, 2004; Bond *et al.*, 2006; Pateras *et al.*, 2006; Yung *et al.*, 2007). SCF^{Skp2} is a ubiquitin E3 ligase complex, with its Skp2 subunit, an F-box protein, providing substrate specificity through direct protein–protein interactions. Skp2 has been shown to promote the G1 to S transition and proliferation in a mouse model (Zhu, 2010). Skp2$^{-/-}$ animals are viable, but cells from mutant mice contain markedly enlarged nuclei with polyploidy and multiple centrosomes (Zhu, 2010). These cells also show reduced growth rate and increased apoptosis. As an important regulator of

cell cycle control, *Skp2* overexpression is a characteristic feature of a variety of cancers (Gstaiger *et al.*, 2001; Signoretti *et al.*, 2002; Ben-Izhak *et al.*, 2003; Wang XC *et al.*, 2012; Wang Z *et al.*, 2012).

Cell cycle progression in *Drosophila* is believed to be controlled by highly conserved cyclins and CDKs (Follette and O'Farrell, 1997). Unlike humans, *Drosophila* has only one known Cip/Kip family member, Dacapo (Dap). Dap negatively regulates the G1 to S transition by inhibiting the CycE/Cdk2 complex, an action that is mediated by the conserved core CDI domain of Dap (de Nooij *et al.*, 1996; Lane *et al.*, 1996). Despite its critical role in cell cycle control, precisely how the stability of Dap protein is regulated is largely unclear. This is in part because Dap appears to have divergent phosphorylation sites critical for ubiquitination (Adams *et al.*, 1996; Morisaki *et al.*, 1997; Huang *et al.*, 2006). Although it was proposed that *CG9772* encodes *Drosophila* Skp2 (dSkp2; Moberg *et al.*, 2004), the genetic and molecular functions of this gene were poorly studied. In a recent report, Ghorbani *et al.* (2011) presented genetic evidence that established a role for *dSkp2* in maintaining diploidy of mitotic cells during development. However, they did not observe a role of dSkp2 in regulating Dap stability, raising the question of whether these two proteins might indeed exhibit a functional relationship that is conserved in cell cycle regulation. Here we describe genetic and molecular studies that specifically investigate the functional relationship between dSkp2 and Dap. Our results show that dSkp2 plays a role in targeting Dap for degradation and has a developmental function interacting with that of Dap in controlling cell cycle progression.

RESULTS

dSkp2 interacts with Dap and has a role in regulating Dap protein level in *Drosophila*

To investigate the question of whether there is a functional relationship between dSkp2 and Dap in *Drosophila*, we determined specifically whether dSkp2 and Dap can physically interact with each other. We transiently expressed tagged proteins 4xMyc-Dap and dSkp2-Flag in *Drosophila* S2 cells and performed coimmunoprecipitation (coIP) assays. We used an anti-Flag antibody to precipitate dSkp2 from the cell extracts and an anti-Myc antibody in Western blots to detect the presence of Dap in the precipitated products. Our results show that 4xMyc-Dap was coimmunoprecipitated when, and only when, dSkp2-Flag was coexpressed in S2 cells (Figure 1A, lane 11; dSkp2–Dap interaction was enhanced by Cks85A, lane 12, a result to which we return in the *Discussion*). These results suggest a physical interaction between dSkp2 and Dap.

The following three sets of experiments performed in S2 cells further suggest that dSkp2 is a component of a conserved SCF E3 ligase complex, SCF^dSkp2, that has a role in targeting Dap for ubiquitination and proteasome-mediated degradation. First, our coIP assays using extracts from S2 cells expressing tagged proteins 4xMyc-SkpA and dSkp2-Flag show that, consistent with the recent report by Ghorbani *et al.* (2011), dSkp2 could physically interact with SkpA, a component of SCF complexes (see Figure 1B and legend for details). Second, the stability of Dap (as Myc-Dap fusion) in S2 cells was sensitive to the proteasome inhibitor epoxomicin (see Figure 1C, lane 3) but not the lysosome inhibitor chloroquine (lane 2; see control in lane 1). Of importance, coexpression of *dSkp2* (as dSkp2-V5 fusion) reduced Dap protein levels in S2 cells (Figure 1D), whereas RNA interference (RNAi) against *dSkp2* increased Dap protein levels (Figure 1E). These results suggest a role of dSkp2 in regulating Dap stability. Third, we expressed tagged proteins Flag-ubiquitin and 4xMyc-Dap in S2 cells, with or without coexpression of

dSkp2-V5. Our results show that coexpression of dSkp2-V5 increased the amount of the polyubiquitinated species of Dap (Figure 1F, lanes 2 and 3), suggesting that dSkp2 has a role in targeting Dap for ubiquitination.

To extend our studies performed in S2 cells and further evaluate the molecular relationship between dSkp2 and Dap, we conducted experiments using *Drosophila* tissue extracts. Here our goal was to use fly tissues as a host to investigate whether these two proteins can also interact as seen in S2 cells. We generated transgenic flies containing UAS-expression constructs for tagged proteins hemagglutinin (HA)-dSkp2 and 4xMyc-Dap. We expressed these proteins in the eye using the *GMR-Gal4* driver, and performed coIP experiments in extracts prepared from the fly heads. We used the anti-Myc antibody to precipitate Dap in head extracts, and used an anti-HA antibody in Western blots to detect the presence of Skp2 in the precipitated products. Our coIP results further confirmed the interaction between dSkp2 and Dap in *Drosophila* tissues (Figure 2A; see lane 9). To evaluate the role of dSkp2 in regulating Dap stability in host tissues of *Drosophila*, we determined the amount of 4xMyc-Dap in the extracts from fly heads with or without coexpression of HA-dSkp2. Our Western blotting results show that coexpression of HA-dSkp2 in the eye reduced the amount of 4xMyc-Dap (Figure 2B, lane 3; see lane 2 as control), whereas coexpression of *dSkp2* RNAi led to an appreciable increase in the amount of 4xMyc-Dap (Figure 2C, lane 2; see lane 1 as control). These results provide further support to our suggestion that Dap stability is regulated by dSkp2.

dSkp2 plays a role in normal wing and eye patterning in *Drosophila*

To investigate the biological significance of the association of dSkp2 with Dap, we analyzed a null allele, *Skp2^ex9*, generated in Andrew Swan's lab (Ghorbani *et al.*, 2011). Our results confirmed the reported early pupal lethality in homozygous animals (data not shown), demonstrating that *dSkp2* is an essential gene for animal survival. To circumvent the lethality problem and facilitate tissue-specific analyses (see later discussion), we evaluated the effects of ubiquitous *dSkp2* knockdown and compared them with those caused by *dSkp2* mutation. Our results show that ubiquitous knockdown of *dSkp2*, using the drivers of *daughterless-Gal4* (*da-Gal4*), *tubulin-Gal4* (*tub-Gal4*), or *actin-GAL4* (*act-Gal4*), led to similar early pupal lethality (data not shown). Of importance, such lethality can be rescued by coexpression of a wt *dSkp2* transgene (data not shown), documenting the specificity of the RNAi lines used in this work.

dSkp2 was also identified recently in a systematic phenotypic screening of *F-box* genes with multiple developmental roles (Dui *et al.*, 2012). Tissue-specific knockdown of *dSkp2*, using two independent RNAi lines, *dSkp2^GD5142* and *dSkp2^KK108837*, caused patterning defects in both the eye and the wing (see Supplemental Figure S1 for the RNAi knockdown efficiency and Supplemental Table S1). *dSkp2* knockdown by RNAi in either the posterior region of the wing (driven by *engrailed-Gal4/en-Gal4*; Figure 3, C′ and C″) or the entire wing (driven by *nubbin-Gal4/nub-Gal4*; Figure 3, B, B′, and B″) led to a wing hair spacing phenotype. In particular, the space between wing hairs became larger, with irregular orientation and frequent clustering of wing hairs (see also Supplemental Figure S2). Furthermore, relative to wild-type or untargeted regions, RNAi-expressing regions became smaller (see Figure 3, B′ and B″, for effects on the entire wing and Figure 3, C′ and C″, for effects on the posterior region). These phenotypes were completely rescued by coexpressing dSkp2 from the transgenes of either *UAS-dSkp2* or *UAS-HA-dSkp2* (Figure 3C and data not shown). Two additional independent RNAi lines, *dSkp2^JF01326* and *dSkp2^HMS00116*, caused similar phenotypes,
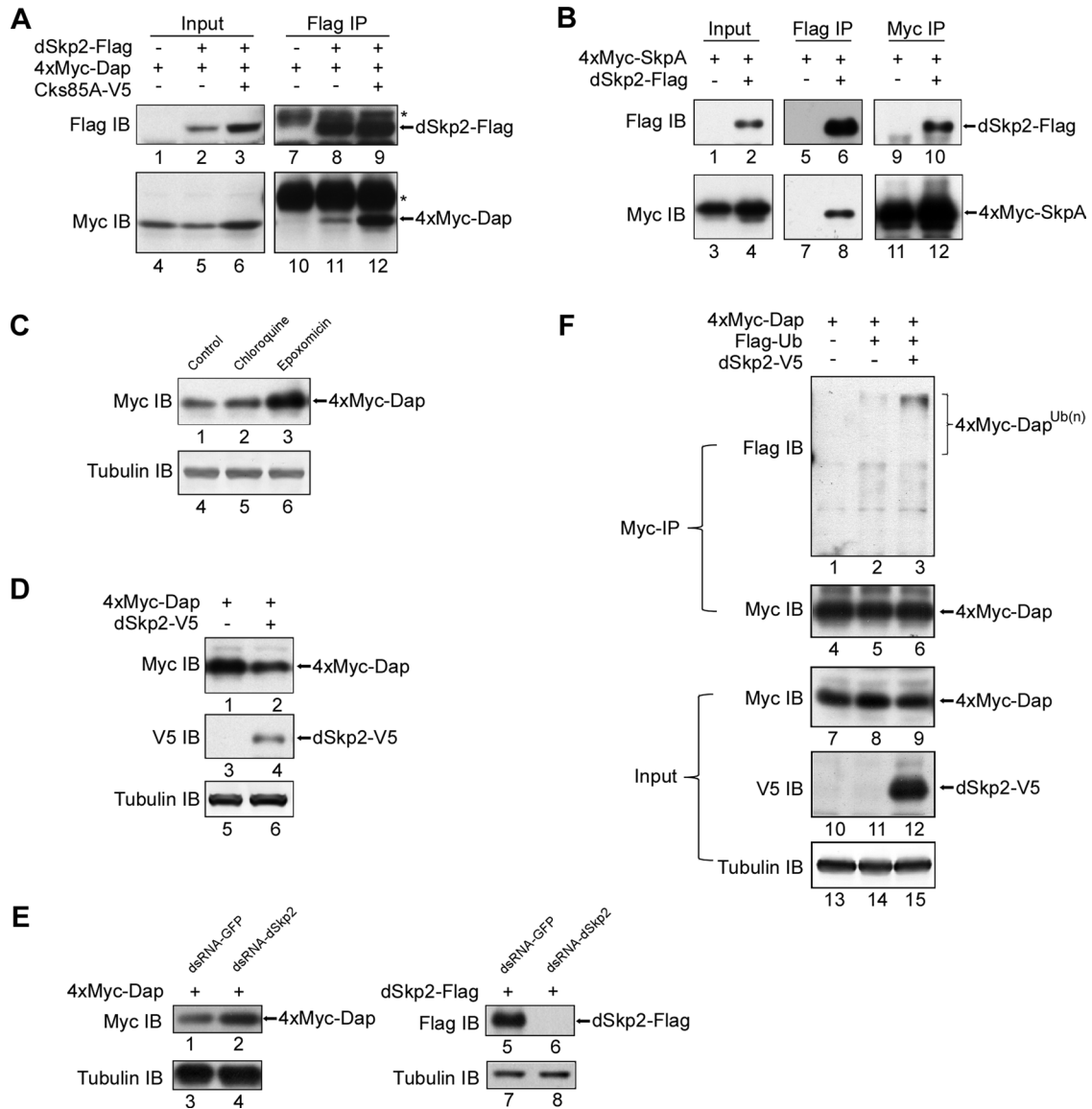
FIGURE 1: dSkp2 interacts with Dap and regulates Dap stability in S2 cells. (A) CoIP between dSkp2 and Dap. S2 cells were transfected with the indicated combination of plasmids. The anti-Flag antibody was used for IP. Antibodies used for immunoblotting (IB) are indicated on the left. Cks85A is the *Drosophila* homologue of Cks1; its expression in S2 cells increased the amount of coIP products (lane 12; see *Discussion*). Asterisk, heavy chain of immunoglobulin G. (B) CoIP between dSkp2 and SkpA. S2 cells were transfected with the indicated combination of plasmids. Anti-Flag antibody (lanes 5–8) or anti-Myc antibody (lanes 9–12) were used for IP, followed by IB using anti-Flag and anti-Myc antibodies to detect dSkp2-Flag and 4xMyc-SkpA, respectively. (C) Dap protein level in S2 cells is sensitive to proteasome inhibitor. S2 cells were transfected with the *4xMyc-dap* plasmid and then treated with the indicated inhibitors (chloroquine and epoxomicin; see the text) for 5 h before cell harvest. Total amount of 4xMyc-Dap in cells was detected by IB using the anti-Myc antibody (lanes 1–3). Tubulin (lanes 4–6) was blotted as loading control. (D) Dap protein level in S2 cells is sensitive to dSkp2 overexpression. S2 cells were cotransfected with the indicated plasmids and cycloheximide (CHX) was added to block translation 5 h before cell harvest. Total protein was detected in IB using the indicated antibodies. Tubulin (lanes 5 and 6) is loading control. (E) S2 cells were first treated with control (*GFP*) dsRNA (lanes 1, 3, 5, and 7) or *dSkp2* dsRNA (lanes 2, 4, 6, and 8) for two times, each lasting 3 d. Cells were then transfected with plasmids expressing 4xMyc-Dap before harvesting (48 h later) for the detection of the total amount of 4xMyc-Dap (lanes 1 and 2). RNAi efficiency was estimated by the reduction in the amount of dSkp2-Flag upon RNAi treatment (lanes 5 and 6). Tubulin (lanes 3, 4, 7, and 8) represents loading control. (F) dSkp2 overexpression enhances the ubiquitination status of Dap. S2 cells were transiently transfected with the indicated plasmids. Whole-cell extracts were prepared for coIP by the anti-Myc antibody. Anti-Flag antibody was used to detect the ubiquitinated species of 4xMyc-Dap as marked. Input represents 1% of the extracts used in coIP.

although with different severity, likely reflecting differences in RNAi strength (Supplemental Table S1). RNAi strength for each of the four lines tested was enhanced by simultaneous overexpression of *dicer2*, an RNAi-machinery protein (Supplemental Table S1). Taken together, these results suggest a role of *dSkp2* in cell proliferation and patterning during *Drosophila* development. The role of *dSkp2*
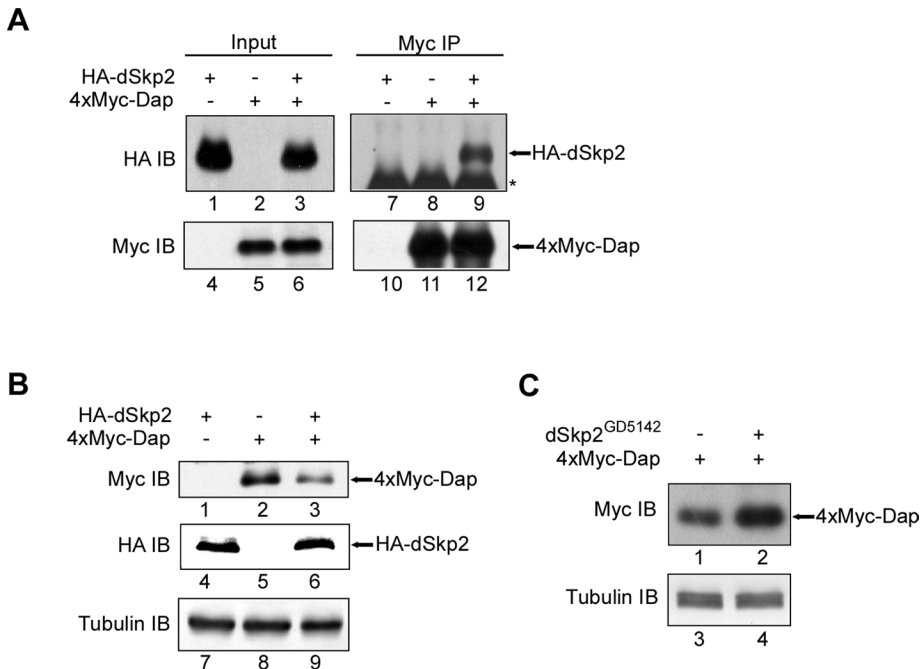
FIGURE 2: dSkp2 interacts with Dap and regulates Dap protein level in *Drosophila* tissues. (A) CoIP analysis detecting dSkp2-Dap interaction. Extracts were prepared from the adult heads of flies with the indicated genotypes: *GMR>HA-dSkp2* (lanes 1, 4, 7, and 10), *GMR>4xMyc-dap* (lanes 2, 5, 8, and 11), and *GMR>HA-dSkp2 + GMR>4xMyc-dap* (lanes 3, 6, 9, and 12). The immunoprecipitates were pulled down with the anti-Myc antibody, and the anti-HA antibody was used in IB to detect the presence of HA-dSkp2. (B) dSkp2 regulates Dap stability. Extracts were prepared from the adult heads of flies as in A. Total protein level in the extracts was detected in IB using the indicated antibodies. Tubulin (lanes 7–9) is loading control. (C) *dSkp2* knockdown in *Drosophila* eyes leads to accumulated Dap proteins in tissue extracts. Extracts were prepared from the adult heads of flies with the indicated genotypes: *GMR>4xMyc-dap* (lanes 1 and 3) and *GMR>4xMyc-dap + GMR>dSkp2^GD5142* (lanes 2 and 4). Myc-tagged Dap protein level was determined by Western blotting using the Myc antibody. Tubulin (lanes 3 and 4) represents loading control.

in patterning was also detectable in the eye, where *dSkp2* knockdown (driven by *eyeless-Gal4/ey-Gal4*) caused rough eyes (Figure 3, A, A′, and A″).

dSkp2 regulates cell cycle progression in *Drosophila* wing discs

To investigate the underlying defects of the wing hair spacing phenotype caused by *dSkp2* knockdown, we determined whether cell number was altered in the adult wing. Supplemental Figure S2 shows that, relative to wild-type wings, *dSkp2* RNAi-treated wings had a significantly reduced number of hairs within areas of the same size, indicating a decrease in cell density. Cell density change has generally been attributed to specific cell cycle alterations that uncouple cell growth from cell division (Weigmann *et al.*, 1997; Neufeld *et al.*, 1998; Swan and Schupbach, 2007). To test this possibility, we measured cell density directly in wing discs that had been stained with 4′,6-diamidino-2-phenylindole (DAPI). As shown in Figure 4, in the posterior region of the wing disc with *dSkp2* knockdown (driven by *en-Gal4*), cell density is significantly lower than the wild-type control (Figure 4, B and C).

Reduced cell density observed in Figure 4 can be explained by a defect in cell cycle progression caused by *dSkp2* knockdown. An alternative (or additional) possibility is that a significant number of cells underwent apoptosis during wing development. It has been documented that cells containing a null allele of *dSkp2*, *dSkp2^ex9*,

exhibit enhanced apoptosis, in addition to other cell cycle defects (Ghorbani *et al.*, 2011). The results shown in Figure 4, A–C, were obtained under a condition that resembles the null allele with respect to the presence of apoptotic cells induced by *dSkp2* RNAi (data not shown). In these experiments, *dicer2* was coexpressed with RNAi expression. We found that, without *dicer2* coexpression, *dSkp2* RNAi did not cause any detectable apoptosis (data not shown). To determine whether weaker perturbations caused by *dSkp2* knockdown are sufficient to affect cell number without crossing the threshold of causing apoptosis, we performed a flip-out analysis (Neufeld *et al.*, 1998) under the condition in which *dicer2* was not coexpressed. As noted by Ghorbani *et al.* (2011), *dSkp2* is located close to the centromere, precluding the use of mitotic recombination to generate *dSkp2* mutant clones. Unlike the fluorescence-activated cell sorting technique, which monitors the snapshot behavior of a group of cells with regard to cell cycle progression, an advantage of the flip-out technique is that it quantifies the "accumulated" outcome of the behavior of cell cycle progression during a period of time. We reasoned that this "compounding effect" (due to time) may permit a sensitive detection of even potentially minor defects in cell cycle progression caused by weaker perturbations.

In our analysis, we used the flip-out technique to generate control (*wild-type*) or RNAi clones that are marked by green fluorescent protein (GFP; Figure 4, D–F; see *Materials and Methods* for details; Neufeld *et al.*, 1998). We induced RNAi clones at 38 h after egg deposition (AED) and allowed animals to develop for another 77 h. We then counted the cells in both wild-type and *dSkp2*-knockdown clones. Figure 4, D′–F′, shows the distributions of clone size expressed as cell number in individual clones analyzed. The average clone sizes for *wild-type*, *dSkp2^KK108837*, and *dSkp2^GD5142* clones were 143, 53, and 26 cells, respectively. On the basis of the measured clone size, we estimated the cell doubling time (see *Materials and Methods*). The estimated doubling times for *wild-type* cells, *dSkp2^KK108837* cells, and *dSkp2^GD5142* cells were 11, 13, and 16 h, respectively. These results support the suggestion that *dSkp2* knockdown can prolong the cell cycle time of wing disc cells.

dSkp2 and *dap* have functions that intersect in controlling cell proliferation

If Dap is indeed a target of SCF^dSkp2, patterning defects caused by reduced dSkp2 activity may be reflective of, at least in part, an increased Dap level in wing cells. To evaluate this possibility, we analyzed whether overexpression of *dap* can cause defects similar to those caused by *dSkp2* knockdown. For this purpose, we used two independent transgenic lines, *UAS-4xMyc-dap* (see earlier discussion) and *UAS-dap^CL660* (Lane *et al.*, 1996). Overexpression of *dap* in wing discs under the control of *en-Gal4* led to a wing hair spacing phenotype (Figure 5A″ and Supplemental Figure 3, C–C′ and
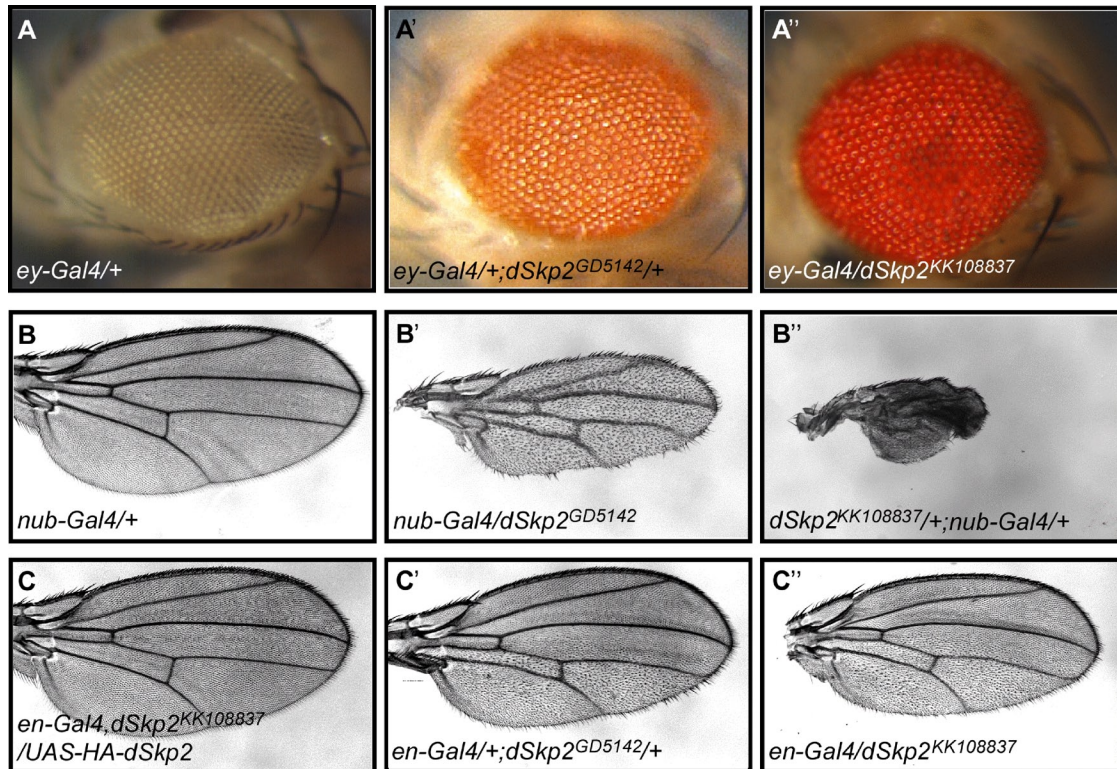
FIGURE 3: Tissue-specific knockdown of *dSkp2* causes developmental defects. (A, A′, and A″) Rough eyes induced by *dSkp2* knockdown in the eye (with the use of the *ey-Gal4* driver). Results from two independent RNAi lines are shown. (B′, B″) *nub-Gal4*-driven expression of these two *dSkp2* RNAi lines in the entire wing results in a similar wing hair spacing phenotype (WHS; see the text for details). Control is shown in B. (C′, C″) *dSkp2* knockdown in the posterior region of the wing (driven by *en-Gal4*) leads to the WHS phenotype in the posterior region only. This phenotype is fully rescued by a simultaneous overexpression of *HA-dSkp2* (C).

D–D″″″). This phenotype is similar to that caused by *dSkp2* knockdown, although with reduced severity (Figure 5A′; see Supplemental Figure S3 for high magnification). We also used other *Gal4* drivers to further evaluate and confirm the phenotypic similarities between *dSkp2* knockdown and *dap* overexpression. Figure 5, B′ and B″, shows that *dSkp2* knockdown or *dap* overexpression, driven by *nub-Gal4* (in the entire wing), led to similar, although differing in severity, wing hair spacing phenotypes and partial loss of the wing margin. In addition, *dSkp2* knockdown or *dap* overexpression, driven by *vg-Gal4* at the D/V boundary of the wing disc, caused a similar wing margin loss phenotype (Figure 5, C and C′). Finally, notum-specific *dSkp2* knockdown or *dap* overexpression, driven by *pnr-Gal4*, gave rise to similar dorsal closure defects and abnormal bristle patterning (Figure 5, D′ and D″). Taken together, these results provide further support to the suggestion that dSkp2 and Dap have regulatory functions in a common pathway(s) during *Drosophila* development.

To further evaluate the functional relationship between *dSkp2* and *dap* in vivo, we performed genetic interaction studies. Here one copy of the mutation, *dap04454* or *dap4*, was introduced into flies that contain an *en-Gal4, dSkp2KK10883* chromosome (Figure 6, C and C′). Our results show that reducing the *dap* gene dose by half was able to partially suppress the wing hair spacing phenotype caused by the *en-Gal4, dSkp2KK108837* chromosome (compare Figure 6, C and C′ with B). These genetic interaction results show that *dSkp2* and *dap* have functions that interact in controlling cell proliferation. This thus led us to examine whether *dSkp2* could also genetically interact with other genes known to be involved in regulating Dap-mediated cell cycle progression.

CycE and Cdk2 are two regulators that promote normal cell cycle in *Drosophila* (Sauer *et al.*, 1995). Knocking down either *CycE* or *Cdk2* in the wing led to a wing hair spacing phenotype similar to that caused by *dSkp2* knockdown (Supplemental Figure S4, C and D). Of importance, overexpression of *CycE* almost completely suppressed the wing hair spacing phenotype caused by *dSkp2* knockdown (Figure 6, D and D′). Taken together, these results show that *dSkp2* genetically interacts with both *dap* and other regulatory genes important for cell proliferation, further supporting a role of dSkp2 in promoting cell cycle progression.

Evaluating the role of dSkp2 in Dap stability at a cellular level in fly tissues

The coIP studies and protein level measurements described in the foregoing suggested a role of dSkp2 in regulating Dap stability (Figures 1, D and E, and 2, B and C). Those experiments required the generation of extracts from cells or tissues and thus were not adequate to give insight into the role of dSkp2 in regulating Dap stability at a cellular level. To further investigate whether the cellular Dap level is subject to dSkp2 regulation, we performed immunostaining studies in the wing disc. We compared the posterior region of the wing discs with or without *dSkp2* knockdown (driven by *en-Gal4*). Dap protein level is uniformly low in wing disc cells (de Nooij *et al.*, 2000). However, *dSkp2* knockdown led to elevated staining of Dap in selected individual cells (Supplemental Figure S5B′; see Supplemental Figure S5A′, control; Supplemental Figure S5C′ shows simultaneous knockdown of *dSkp2* and *Cks85A* with an enhanced effect; see *Discussion* for further information).
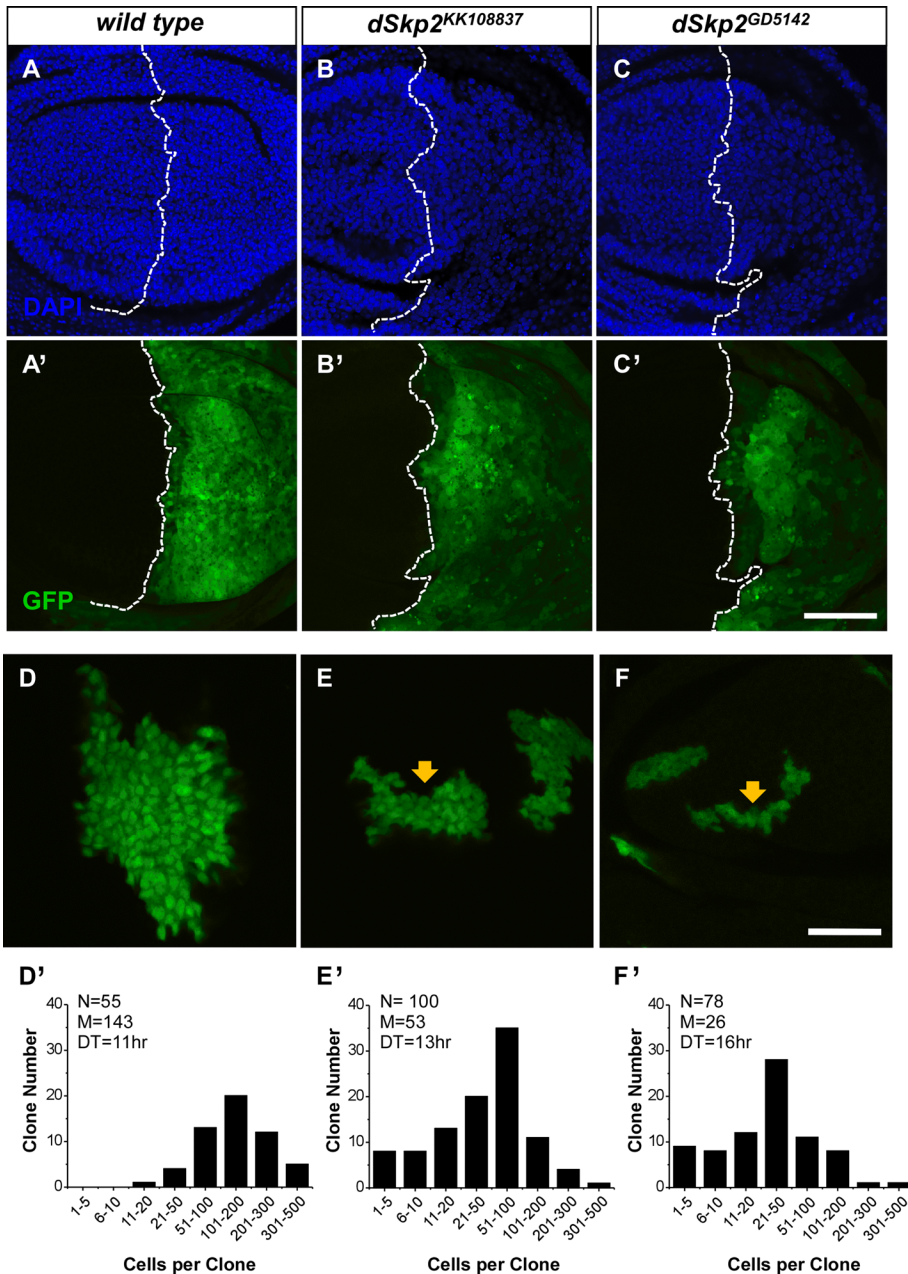
FIGURE 4: Knockdown of *dSkp2* slows cell proliferation in the wing discs. (A–C) DAPI staining of wing imaginal discs showing nuclear density differences in the posterior region of the disc with (B, C) or without (A) *dSkp2* knockdown (driven by *en-Gal4* in combination with *UAS-dcr2* at 29°C). GFP signals mark the expression domain of *en-Gal4* (B', C'). (A') The *en-Gal4, UAS-GFP* control. The genotypes are *UAS-dcr2/+; en-Gal4, UAS-GFP/+* (A, A'), *UAS-dcr2/+; en-Gal4, UAS-GFP/dSkp2^{KK108837}* (B, B'), and *UAS-dcr2/+; en-Gal4, UAS-GFP/+; dSkp2^{GD5142}/+* (C, C'). Scale bar, 50 μm. (D–F) Cell division rate is decreased by *dSkp2* knockdown (E, F), and GFP signals mark the RNAi-expressing clones (see the text for details), leading to smaller clones (arrows in E and F). In D, the GFP-marked cells are *wild type*. (D'–F') Bar graphs showing the distribution of clones with different cell number per clone. *N*, number of total clones counted; *M*, median cell number per clone; *DT*, doubling time. The genotypes are *y w, hs-flp/+; Act>y+>Gal4, UAS-GFP/+* (D and D'), *y w, hs-flp/+; Act>y+>Gal4, UAS-GFP/dSkp2^{KK108837}* (E, E'), and *y w, hs-flp/+;Act>y+>Gal4, UAS-GFP/+; dSkp2^{GD5142}/+* (F, F'). Scale bar, 25 μm.

likely a contributing factor for the relatively modest effects of *dSkp2* knockdown on Dap levels under the experimental conditions. To get around this technical limitation and increase the detection sensitivity for an improved evaluation of the role of dSkp2 in regulating Dap stability at a cellular level, we took advantage of *UAS-4xMyc-dap* transgenic lines and used an anti-Myc antibody in our immunostaining assays. We approached this problem by analyzing the effects of either knockdown or overexpression of *dSkp2* on the detected signals for 4xMyc-Dap in wing discs. For each set of experiments, we ensured that all the experimental and imaging steps were performed side by side to allow effective comparisons. Figure 7, A'–C', shows immunostained wing discs that express, respectively, *4xMyc-dap* alone, *4xMyc-dap* together with *dSkp2* knockdown, and *4xMyc-dap* together with *dSkp2* and *Cks85A* knockdown. Expression of 4xMyc-Dap alone led to accumulations of the protein in a nonuniform manner among the wing disc cells (Figure 7A'). With *dSkp2* knockdown, we detected a significant increase in both the mean number of fluorescence intensity clusters (referred to as intensity dots) within the *4xMyc-dap* expression domain of the disc and the mean aggregate intensity of these dots (see Figure 7, D and E, for further increase caused by simultaneous knockdown of *Cks85A*). Conversely, coexpression of *HA-dSkp2* led to significant reduction in these quantities (Figure 7, H and I). Taken together, these results provide further in vivo evidence supporting our suggestion that Dap is a substrate of SCF^{dSkp2} in manifesting the patterning defects caused by reduction in dSkp2 activity during development.

DISCUSSION

Despite extensive studies of human Skp2 since its discovery more than a decade ago, the role of *Drosophila* Skp2 (dSkp2) has not been fully characterized. It is logical to infer that, for a highly conserved and fundamental process such as cell cycle control, the basic structure of the regulatory networks is most likely conserved among different species. However, it is unresolved whether the functional relationship between dSkp2 and its inferred target Dap is indeed conserved (see *Introduction*). In particular, a recent study raised the question of whether dSkp2 has a role in regulating Dap stability (Ghorbani *et al.*, 2011). Our study was designed to shed light on this specific question. We provide both in vitro and in vivo evidence that documents a role of dSkp2 in targeting Dap for ubiquitination and degradation and in regulating cell cycle progression. Our conclusion regarding the role of dSkp2 in regulating Dap stability differs

Low levels of the endogenous Dap in wild-type (wt) wing discs are difficult to detect by the antibody we used (de Nooij *et al.*, 2000). In the experiments shown in Supplemental Figure S5, the uniformly low levels of Dap in wt wing discs are probably not beyond experimental background levels. This technical limitation is
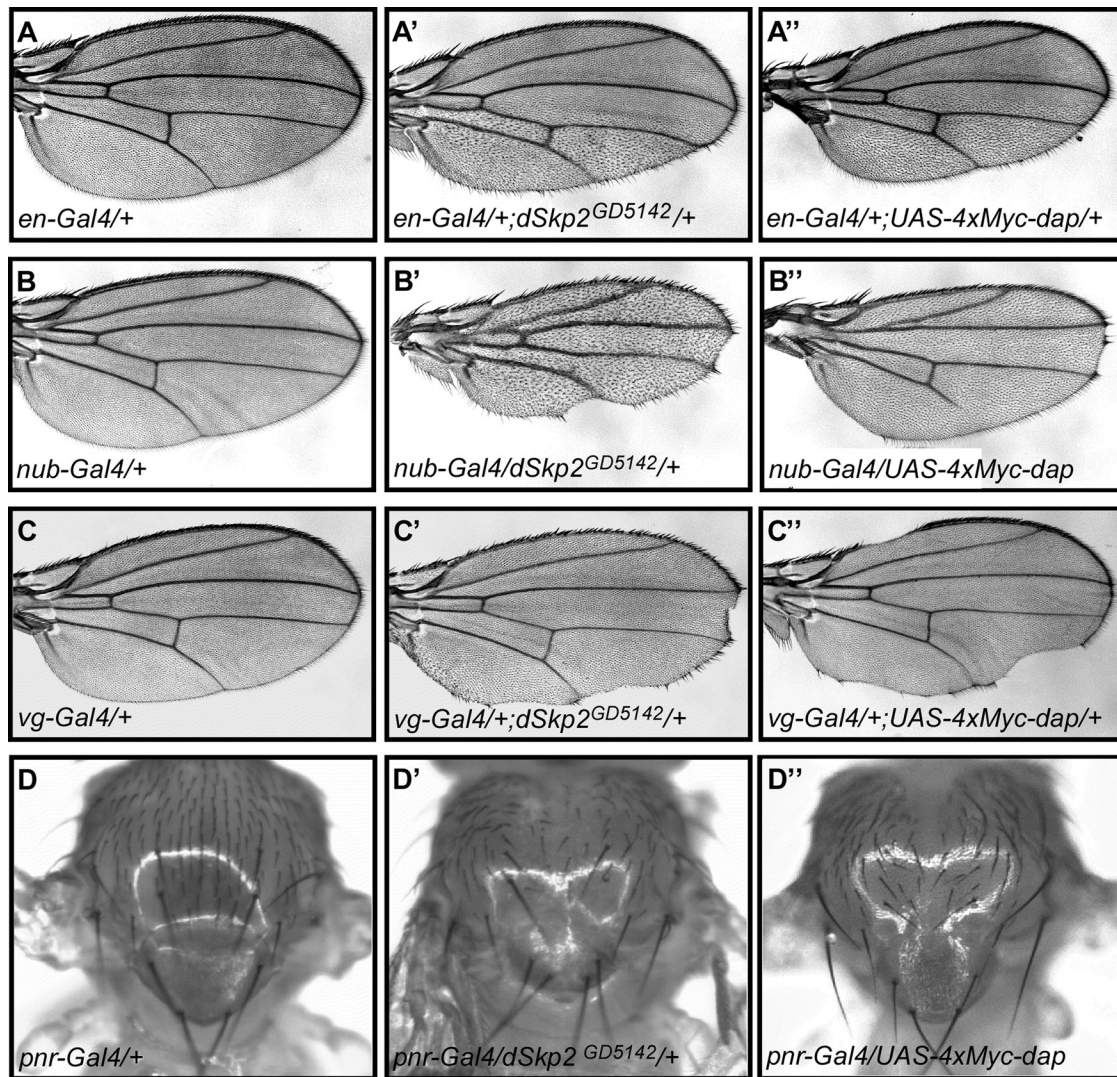
FIGURE 5: Similar phenotypes caused by *dap* overexpression and *dSkp2* knockdown. Light microscopic images showing wings (A, A', and A''; B, B', and B''; C, C', and C'') and nota (D, D', and D'') from flies with the indicated genotypes. (A) A control wing of *en-Gal4*. (A', A'') Wings exhibiting the WHS phenotype (with different severity) in the posterior regions, caused by either *dSkp2* knockdown (A') or *dap* overexpression (A''), each under the control of *en-Gal4*. (B) A control wing of *nub-Gal4*. (B', B'') Wings showing the WHS phenotype in the entire wing by either *dSkp2* knockdown (B') or *dap* overexpression (B'') under the control of *nub-Gal4*. (C) A control wing of *vg-Gal4*. (C', C'') Wings showing nicking phenotype on the wing margin (arrows), caused by either *dSkp2* knockdown (C') or *dap* overexpression (C'') under the control of *vg-Gal4*. (D) A control notum of *pnr-Gal4*. (D', D'') Nota displaying dorsal closure defects and loss of bristles by either *dSkp2* knockdown (D') or overexpression of *dap* (D'') under the control of *pnr-Gal4*.

from that of Ghorbani *et al.* (2011), likely reflecting differences in detection method or sensitivity, as opposed to the way in which *dSkp2* is perturbed. The *dSkp2*-null allele and the RNAi lines used in this study had identical phenotypes and, of importance, the *dSkp2*-knockdown phenotypes can be fully rescued by wild-type *dSkp2*. Because *Skp2* has been associated with multiple cancers (see *Introduction*), our study thus suggests that *Drosophila* as a model system may benefit future studies of Skp2-mediated human tumors (Gstaiger *et al.*, 2001; Signoretti *et al.*, 2002; Ben-Izhak *et al.*, 2003; Wang XC *et al.*, 2012; Wang Z *et al.*, 2012).

The conservation between the Dap/p21-mediated cell cycle control networks in humans and flies extends to the function of Cdc kinase subunit 1 (Cks1) in regulating Dap/p21 protein level. Cks1 is a small accessory protein that facilitates SCF^{Skp2} in targeting its substrates for degradation (Ganoth *et al.*, 2001; Mongay *et al.*, 2001; Spruck *et al.*, 2001; Wang *et al.*, 2003, 2004; Hao *et al.*, 2005; Yao *et al.*, 2006). The *Drosophila* homologue of Cks1, Cks85A, was recently shown to interact with dSkp2 and play an important role in development (Ghorbani *et al.*, 2011). In our study, knockdown of *Cks85A* and *dSkp2* caused a similar wing hair spacing phenotype (Supplemental Figure S4B). Simultaneous knockdown of *dSkp2* and *Cks85A* led to more pronounced accumulations of the endogenous Dap protein relative to *dSkp2* or *Cks85A* knockdown alone (Supplemental Figure S5 and data not shown). Because the physical interaction between dSkp2 and Dap is enhanced by Cks85A (Figure 1A, lane 12), Cks85A most likely achieves its biological functions through a conserved molecular mechanism of strengthening the interaction between SCF^{Skp2} and its substrates (Ganoth *et al.*, 2001; Spruck *et al.*, 2001).
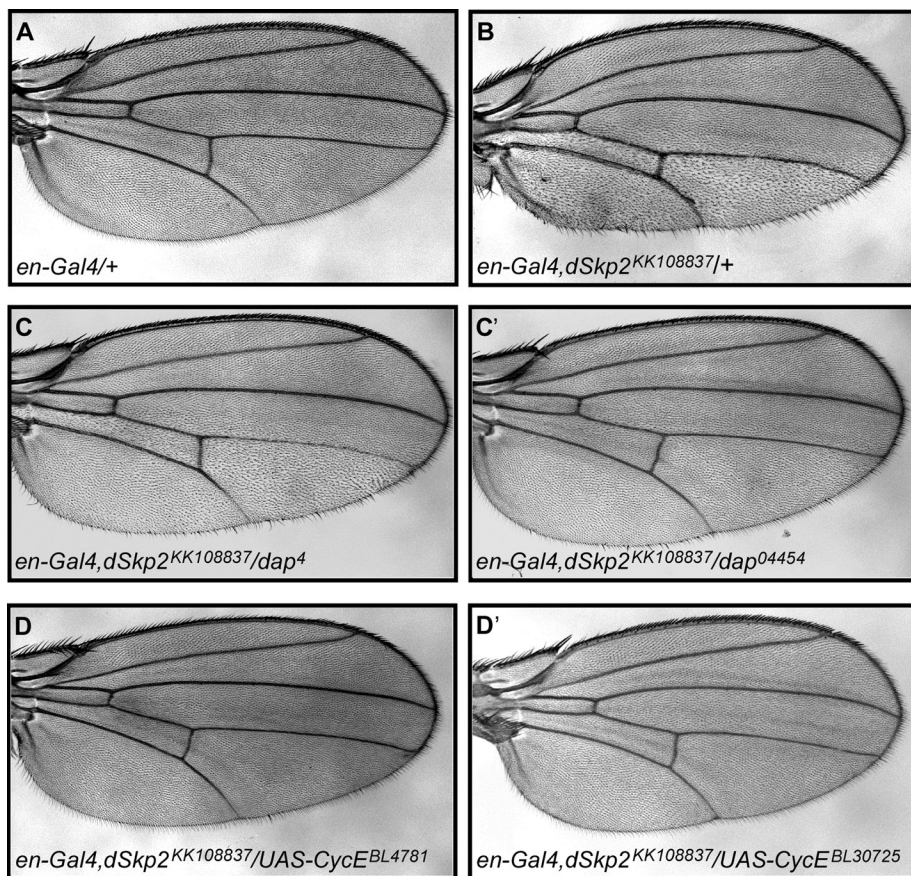
FIGURE 6: *dSkp2* genetically interacts with *dap* and *CycE* in the *Drosophila* wing. (A) A control wing of *en-Gal4*. (B) *dSkp2* knockdown in the posterior region of the wing under the control of *en-Gal4* leads to the typical WHS phenotype. Introducing a mutant copy of either *dap04454* (C) or *dap4* (C') into the *en>dSkp2KK108837* flies partially suppresses the WHS phenotype. Overexpression of CycE from *UAS-CycE* (D, D', two independent transgenes) almost completely rescues the WHS phenotype caused by *en>dSkp2KK108837*.

enhanced apoptosis are two aspects of altered cellular behavior that respond to two distinct thresholds of *dSkp2* activity alterations in the wing disc (Figure 4).

In humans, p21[cip1] has been shown to undergo proteasome-mediated degradation through the actions of at least two E3 ligases, CRL4[Cdt2] and SCF[Skp2]. Whereas CRL4[Cdt2] predominantly regulates p21 levels during the S phase, SCF[Skp2]-mediated degradation of p21 does not have such a temporal restriction. In *Drosophila*, Dap protein level is known to oscillate during ovarian endocycles (de Nooij *et al.*, 2000). In our experiments, the heterogeneity in 4xMyc-Dap staining in the wing disc is not abolished by dSkp2 activity alterations (Figure 7), suggesting that Dap may also be targeted for degradation by multiple E3 ligases and that dSkp2 may not be primarily responsible for its oscillating property. Finally, the E3 ligase complex of Cul4-DDB1-Cdt2 is conserved in *Drosophila* (Zielke *et al.*, 2011), and a loss of Cul-4 based E3 ligases causes a G1 arrest in a manner that is dependent on Dap (Higa *et al.*, 2006). These results suggest that Dap stability may also be subject to regulation by Cul-4 E3 ligases. Understanding the complete fine structure of the regulatory networks for cell cycle control and their roles during development remains an interesting scientific problem and long-term challenge. The present study, which documents the dSkp2–Dap connection, represents an important step toward meeting this challenge through the use of a genetic model system.

MATERIALS AND METHODS

Drosophila strains used in this study are listed according to their sources (see foregoing text for references to individual stocks/mutations):

Vienna *Drosophila* RNAi Center (Vienna, Austria): *dSkp2GD5142*, *dSkp2KK108837*, *Cks85AGD13737*.

Bloomington *Drosophila* Stock Center (Bloomington, IN): *w*;dap4/CyO*, *dap04454/CyO*, *dSkp2JF01326*, *dSkp2HMS00116*, *Cdk2HMS00174*, *w;UAS-CycE.L*, *w*;UAS-CycE.R*, *UAS-dcr2 w1118*; *en-Gal4 UAS-GFP, UAS-dcr2 w1118;nub-Gal4, UAS-dcr2 w1118;pnr-Gal4*.

National Institute of Genetics (Mishima, Japan): *CycE-IR*.

Christian F. Lehner (University of Zurich, Switzerland): *UAS-DapCL659* and *UAS-DapCL660* transgenic flies.

Andrew Swan (University of Windsor, Canada): *dSkp2ex9* mutant.

Flies were reared under standard condition at 25°C unless stated otherwise.

Generation of transgenic flies

To construct *pUAST-dSkp2*, two PCR fragments amplified from *dSkp2/CG9772* genomic DNA were obtained using the following primers: 5'-ataagaat**GCGGCCGC**AGCGCGAAGTTTTTGTGTTT-3'

It is well documented that E3 ligases can have multiple substrate proteins and a given protein can be targeted for degradation by multiple E3 ligases (Skaar *et al.*, 2009a,b; Dui *et al.*, 2012). These particular features of the E3 ligase–substrate relationship contribute significantly to the richness of the biological regulatory systems. In addition to p21[cip1]/p27[kip1]/p57[kip2], human Skp2 can also target other proteins for degradation, including CycA (Yam *et al.*, 1999; Ji *et al.*, 2006), CycD1 (Ganiatsas *et al.*, 2001), Cdk9 (Kiernan *et al.*, 2001), CycE (Yeh *et al.*, 2001), pRb[p130] (Tedesco *et al.*, 2002; Bhattacharya *et al.*, 2003), Myc (Kim *et al.*, 2003; von der Lehr *et al.*, 2003), and Cdt1 (Li *et al.*, 2003). Thus it is likely that dSkp2 may also have multiple substrates to execute the various biological functions of dSkp2. For example, it remains possible that, in addition to Dap, dSkp2 may also have a role in regulating the activity and/or stability of Cdt1/Dup in *Drosophila* and contribute to the development of polyploidy cells. It has been reported that overexpression of *Drosophila* Cdt1/dup (*double-parked*) is sufficient to induce rereplication (Whittaker *et al.*, 2000; Thomer *et al.*, 2004; May *et al.*, 2005; Lin *et al.*, 2009). Future studies with sensitive tools are required to further investigate whether there might be a functional relationship between *dSkp2* and *Cdt1/dup* and, if there is, the disentangled molecular and genetic relationships among all the relevant regulators in maintaining diploidy in mitotic cells (Ghorbani *et al.*, 2011). We note that, despite the complexity of the regulatory roles of dSkp2 during development, an important finding of our study is that the defects in cell cycle progression and

FIGURE 7: dSkp2 has a role in regulating Dap protein level in vivo. (A–E) Knockdown of *dSkp2* leads to an increase in fluorescence signals for 4xMyc-Dap in wing discs. *4xMyc-dap⁵¹* was expressed in the posterior regions of the wing discs under the control of *en-Gal4* either alone (A, A') or with the *dSkp2* knockdown (B, B') or with a simultaneous knockdown of *dSkp2* and *Cks85A* (C, C'). The confocal images shown were from side-by-side experiments and were captured under identical imaging settings. (D, E) Mean number of clusters of fluorescence

(*Not*I site in bold capitals, ATG codon of *dSkp2* coding sequence is after this primer) and 5′-TGGAAGCCATACTCAGGTCA-3′ for fragment 1, 5′-TAAGTGGCTCCCGAA-GAAGA-3′ and 5′-ctag**TCTAGA**CGCAG-CAAAACAAATTCAAA-3′ (*Xba*I site in bold capitals) for fragment 2. After cutting with *Not*I/*Xho*I and *Xho*I/*Xba*I, two fragments were ligated into the *Not*I/*Xba*I sites of the *pUAST* vector. To construct *pUAST-HA-dSkp2*, a modified *pUAST* vector with ATG start codon and HA tag sequence at the *Eco*RI site (Huang *et al.*, 2011) was used. To construct the fusion gene encoding the HA-tagged dSkp2 protein, another pair of primers for PCR fragment 3 was used: 5′-ataagaat**GCGGCCGC**GGAGCAGTCG-CAAGCACAG-3′ (*Not*I site in bold capitals) and 5′-TGGAAGCCATACTCAGGTCA-3′. Fragment 3, which was cut with *Not*I/*Xho*I, and the aforementioned fragment 2, which was cut with *Xho*I/*Xba*I, were ligated into *Not*I/*Xba*I linearized *pUAST-HA* vector. To construct *pUAST-4xMyc-Dap*, another modified *pUAST* vector (kindly provided by Jianming Chen, Xiamen University, China) with 4xMyc tag sequence inserted at *Bgl*II/*Kpn*I site was used. A PCR fragment containing the entire coding region (except for the ATG start codon) was obtained using the following primers: 5′-ctag-**TCTAGA**GGTCAGTGCCCGAGTCCT-3′ (*Xba*I site in bold capitals) and 5′-ctag**TCTA-GA**CCAGCGAATCTGGAGCATTA-3′ (*Xba*I site in bold capitals). After cutting with *Xba*I, the PCR fragment was cloned into the *Xba*I site of the *pUAST-4xMyc* vector, and clones with correct orientation were picked up for sequencing verification. Correct constructs with sequence confirmation of *pUAST-dSkp2*, *pUAST-HA-dSkp2*,

signals (referred to as dots) per disc and mean aggregate intensity (in arbitrary units), respectively, of the detected dots. Error bars, SD calculated across different discs in a group. *n* = 20 discs for each genotype. (F–I) Coexpression of *HA-dSkp2* leads to a reduction in fluorescence signals for 4xMyc-Dap in wing discs. *4xMyc-dap¹⁰⁻¹* was expressed in the posterior region of the wing discs under the control of *en-Gal4* either alone (F, F') or with *HA-dSkp2* together (G, G'). The confocal images shown were based on side-by-side experiments with images captured under identical settings. (H,I) Mean number of fluorescent dots detected per disc and mean aggregate intensity (in arbitrary units) of the detected dots, respectively. *n* = 13 for *4xMyc-dap¹⁰⁻¹* discs and 19 for *4xMyc-dap¹⁰⁻¹&HA-dSkp2* discs. **p < 0.01 (Student's *t* test). Scale bar, 75 µm.

and *pUAST-4xMyc-Dap* were used for microinjection to generate transgenic flies, using standard protocols (Xu *et al.*, 2009; Chen *et al.*, 2010).

Constructs for protein expression in S2 cells, transfection, and RNA interference assays

The *pAc5.1/V5-His* vector with the *Drosophila actin* 5C promoter was used for protein expression in S2 cells (Liu and Ma, 2011). Plasmids of *pAc5.1-dSkp2-FLAG*, *pAc5.1-dSkp2-V5*, *pAc5.1–4xMyc-Dap*, *pAc5.1–4xMyc-SkpA*, and *pAc5.1-Cks85A-V5* were constructed by standard cloning methods (cloning strategies are available upon request). *Drosophila* S2 cells were cultured in Hyclone serum-free insect cell culture medium (Roche, Indianapolis, IN). Transfection of S2 cells was performed using FuGENE HD transfection reagent (Roche) according to the manufacturer's instructions. For treating S2 cells, the proteasome inhibitor epoxomicin (final concentration 300 nM; Sigma-Aldrich, St. Louis, MO), the lysosome inhibitor chloroquine diphosphate (final concentration 500 μM; Sigma-Aldrich), and the translation inhibitor cycloheximide (final concentration 100 μg/ml; Sigma-Aldrich) were used. For RNA interference, double-strand RNA (dsRNA) was prepared with the RiboMAX large-scale RNA Production System-T7 Kit (Promega, Madison, WI). The primers for GFP control were 5′-ttaatacgactcactatagggggagaATGGTGAGCAAGGGCGAGGAGCTG-3′ (forward) and 5′-ttaatacgactcactatagggggagaCTTGTACAGCTCGTCCATGCCGAGAG-3′ (reverse). The primers for *dSkp2* RNAi were 5′-*aatt*ctaatacgactcactatagggggagaCTCAATTTTCAGCCATCAACCAGCA-3′ (forward) and 5′-*aatt*ctaatacgactcactatagggggagaCAAGGACTCCCCGCCGTACAA-3′ (reverse). For a 12-well plate, 1 ml of culture medium in each well was treated with 7.5 μg of dsRNA for 3 d before plasmid transfection.

Coimmunoprecipitation assays

S2 cells were transfected or cotransfected with plasmids that express a desired combination of proteins. Cell lysates were prepared in IP lysis buffer (50 mM Tris-HCl, 120 mM NaCl, 0.2 mM EDTA, 0.2 mM ethylene glycol tetraacetic acid, 0.4% NP40, 0.4% sodium deoxycholate), followed by ultrasonication treatment: 100 Hz, 4 s with 6-s interval, 10 times. For coIP assays with *Drosophila* tissue extracts, >500 adult fly heads were collected and homogenized in the same IP lysis buffer as used for the S2 cells. The prepared cell or tissue lysates were incubated with specific antibody and protein A/G agarose (Abmart, Shanghai, China) before proper centrifugation and buffer washes. Immunoprecipitates were resolved by SDS–PAGE, and Western blots were performed using appropriate antibodies according to standard protocols (Wei *et al.*, 2008, 2010). Input lanes represent 1% of the total lysates used in coIP reactions unless stated otherwise. The loading of the immunoprecipitated products was identical for all lanes, each representing 15% of these products.

Immunocytochemistry

Wandering third-instar larvae with correct genotypes were collected and dissected in cold phosphate-buffered saline (PBS). Imaginal discs were fixed in 3.7% paraformaldehyde in PBS for 20 min. After four washes in PBS with 0.3% Triton X-100, 5% normal horse serum in PBS/Tween-20 was used for 15 min preblocking. The discs were then incubated with different primary antibodies (see later description) overnight at 4°C. Subsequently, corresponding fluorescent secondary antibodies were used for signal detection. All confocal images were captured using a Leica confocal microscope SP5 (Leica, Wetzlar, Germany) as described previously (Liu *et al.*, 2011; Xie *et al.*, 2012). All confocal images shown were captured under identical settings, each representing data from a single *z*-section.

Cell proliferation rate estimates

Wild-type, *dSkp2^{KK108837}*, and *dSkp2^{GD5142}* clones were induced by the FRT (Flippase recognition target)-mediated "flip-out" method. The strain *y w, hs-flp; Act>y^{+}>Gal4, UAS-GFP* was used for this purpose (Neufeld *et al.*, 1998). Larvae of each genotype were heat shocked at 38 ± 1 h AED for 1 h at 37°C, and wing imaginal discs were dissected and fixed at 115 h AED (Neufeld *et al.*, 1998). Clones marked by GFP-positive signals were imaged under a Leica confocal microscope SP5. Cells per clone were counted from 17 discs of *wild type*, 21 discs of *dSkp2^{KK108837}*, and 13 discs of *dSkp2^{GD5142}*. Median cell number per clone is taken as M, and cell doubling time (DT) was calculated as $DT = T/\log_2 M$ ($T = 77$ h in this study).

Primary and secondary antibodies

The primary antibodies were diluted to 1:100 for immunofluorescence assays and 1:5000 for Western blotting. Antibodies used in this study were as follows: rabbit anti–c-Myc (Sigma-Aldrich); mouse anti–c-Myc (CWBIO, Beijing, China); mouse anti-V5 (Invitrogen, Carlsbad, CA); mouse anti-HA (Abmart); mouse anti-Dap (1:5 dilution; DSHB-NP1; Developmental Studies Hybridoma Bank, University of Iowa, Iowa City, IA); mouse anti-Flag (Sigma-Aldrich); and anti-tubulin (CWBIO). For Western blotting, horseradish peroxidase–linked secondary antibodies (1:5000 dilution) were used. For immunostaining assays, the corresponding fluorescent secondary antibodies (fluorescein isothiocyanate, tetramethylrhodamine isothiocyanate, or Cy5) were used in 1:400 dilution.

Quantification of fluorescence signals for 4xMyc-tagged Dap in wing discs

Quantification of the fluorescence signals for 4xMyc-tagged Dap was performed to evaluate both the number of fluorescent clusters (referred to as dots) in a disc and the aggregate intensity (in arbitrary units) of the detected dots. Briefly, for each image, we first used DAPI counterstain signals to mask the disc. Whenever necessary, we performed manual cropping to remove the conjugated, unwanted tissues or other discs present in an image. We then used the Otsu thresholding algorithm (Otsu, 1979; Cheung *et al.*, 2011) to define a threshold. Clusters of fluorescence intensity signals above this threshold were identified, and the number was determined for each disc. The aggregate intensities (in arbitrary units) of individual dots were also calculated, and a mean was calculated for all the detected dots in each disc. All calculations were performed on MATLAB (MathWorks, Natick, MA).

REFERENCES

Adams PD, Sellers WR, Sharma SK, Wu AD, Nalin CM, Kaelin WG Jr (1996). Identification of a cyclin-cdk2 recognition motif present in substrates and p21-like cyclin-dependent kinase inhibitors. Mol Cell Biol 16, 6623–6633.

Amati B, Vlach J (1999). Kip1 meets SKP2: new links in cell-cycle control. Nat Cell Biol 1, E91–E93.

Ben-Izhak O, Lahav-Baratz S, Meretyk S, Ben-Eliezer S, Sabo E, Dirnfeld M, Cohen S, Ciechanover A (2003). Inverse relationship between Skp2 ubiquitin ligase and the cyclin dependent kinase inhibitor p27Kip1 in prostate cancer. J Urol 170, 241–245.

Bhattacharya S, Garriga J, Calbo J, Yong T, Haines DS, Grana X (2003). SKP2 associates with p130 and accelerates p130 ubiquitylation and degradation in human cells. Oncogene 22, 2443–2451.

Bond M, Sala-Newby GB, Wu YJ, Newby AC (2006). Biphasic effect of p21Cip1 on smooth muscle cell proliferation: role of PI 3-kinase and Skp2-mediated degradation. Cardiovasc Res 69, 198–206.

Carrano AC, Eytan E, Hershko A, Pagano M (1999). SKP2 is required for ubiquitin-mediated degradation of the CDK inhibitor p27. Nat Cell Biol 1, 193–199.

Chen Y, Dui W, Yu Z, Li C, Ma J, Jiao R (2010). *Drosophila* RecQ5 is required for efficient SSA repair and suppression of LOH in vivo. Protein Cell 1, 478–490.

Cheung D, Miles C, Kreitman M, Ma J (2011). Scaling of the Bicoid morphogen gradient by a volume-dependent production rate. Development 138, 2741–2749.

de Nooij JC, Graber KH, Hariharan IK (2000). Expression of the cyclin-dependent kinase inhibitor Dacapo is regulated by cyclin E. Mech Dev 97, 73–83.

de Nooij JC, Letendre MA, Hariharan IK (1996). A cyclin-dependent kinase inhibitor, Dacapo, is necessary for timely exit from the cell cycle during *Drosophila* embryogenesis. Cell 87, 1237–1247.

Dui W, Lu W, Ma J, Jiao R (2012). A systematic phenotypic screen of F-box genes through a tissue-specific RNAi-based approach in *Drosophila*. J Genet Genomics 39, 397–413.

Follette PJ, O'Farrell PH (1997). Cdks and the *Drosophila* cell cycle. Curr Opin Genet Dev 7, 17–22.

Ganiatsas S, Dow R, Thompson A, Schulman B, Germain D (2001). A splice variant of Skp2 is retained in the cytoplasm and fails to direct cyclin D1 ubiquitination in the uterine cancer cell line SK-UT. Oncogene 20, 3641–3650.

Ganoth D, Bornstein G, Ko TK, Larsen B, Tyers M, Pagano M, Hershko A (2001). The cell-cycle regulatory protein Cks1 is required for SCF(Skp2)-mediated ubiquitinylation of p27. Nat Cell Biol 3, 321–324.

Ghorbani M, Vasavan B, Kraja E, Swan A (2011). Cks85A and Skp2 interact to maintain diploidy and promote growth in *Drosophila*. Dev Biol 358, 213–223.

Gstaiger M, Jordan R, Lim M, Catzavelos C, Mestan J, Slingerland J, Krek W (2001). Skp2 is oncogenic and overexpressed in human cancers. Proc Natl Acad Sci USA 98, 5043–5048.

Hao B, Zheng N, Schulman BA, Wu G, Miller JJ, Pagano M, Pavletich NP (2005). Structural basis of the Cks1-dependent recognition of p27(Kip1) by the SCF(Skp2) ubiquitin ligase. Mol Cell 20, 9–19.

Higa LA, Yang X, Zheng J, Banks D, Wu M, Ghosh P, Sun H, Zhang H (2006). Involvement of CUL4 ubiquitin E3 ligases in regulating CDK inhibitors Dacapo/p27Kip1 and cyclin E degradation. Cell Cycle 5, 71–77.

Huang H, Du G, Chen H, Liang X, Li C, Zhu N, Xue L, Ma J, Jiao R (2011). *Drosophila* Smt3 negatively regulates JNK signaling through sequestering Hipk in the nucleus. Development 138, 2477–2485.

Huang H, Regan KM, Lou Z, Chen J, Tindall DJ (2006). CDK2-dependent phosphorylation of FOXO1 as an apoptotic response to DNA damage. Science 314, 294–297.

Ji P, Goldin L, Ren H, Sun D, Guardavaccaro D, Pagano M, Zhu L (2006). Skp2 contains a novel cyclin A binding domain that directly protects cyclin A from inhibition by p27Kip1. J Biol Chem 281, 24058–24069.

Kiernan RE, Emiliani S, Nakayama K, Castro A, Labbe JC, Lorca T, Nakayama Ki K, Benkirane M (2001). Interaction between cyclin T1 and SCF(SKP2) targets CDK9 for ubiquitination and degradation by the proteasome. Mol Cell Biol 21, 7956–7970.

Kim SY, Herbst A, Tworkowski KA, Salghetti SE, Tansey WP (2003). Skp2 regulates Myc protein stability and activity. Mol Cell 11, 1177–1188.

Kossatz U, Dietrich N, Zender L, Buer J, Manns MP, Malek NP (2004). Skp2-dependent degradation of p27kip1 is essential for cell cycle progression. Genes Dev 18, 2602–2607.

Lane ME, Sauer K, Wallace K, Jan YN, Lehner CF, Vaessin H (1996). Dacapo, a cyclin-dependent kinase inhibitor, stops cell proliferation during *Drosophila* development. Cell 87, 1225–1235.

Li X, Zhao Q, Liao R, Sun P, Wu X (2003). The SCF(Skp2) ubiquitin ligase complex interacts with the human replication licensing factor Cdt1 and regulates Cdt1 degradation. J Biol Chem 278, 30854–30858.

Lin HC, Wu JT, Tan BC, Chien CT (2009). Cul4 and DDB1 regulate Orc2 localization, BrdU incorporation and Dup stability during gene amplification in *Drosophila* follicle cells. J Cell Sci 122, 2393–2401.

Liu J, Ma J (2011). Fates-shifted is an F-box protein that targets Bicoid for degradation and regulates developmental fate determination in *Drosophila* embryos. Nat Cell Biol 13, 22–29.

Liu J, Wu Q, He D, Ma T, Du L, Dui W, Guo X, Jiao R (2011). *Drosophila* sbo regulates lifespan through its function in the synthesis of coenzyme Q in vivo. J Genet Genomics 38, 225–234.

May NR, Thomer M, Murnen KF, Calvi BR (2005). Levels of the origin-binding protein Double parked and its inhibitor Geminin increase in response to replication stress. J Cell Sci 118, 4207–4217.

Moberg KH, Mukherjee A, Veraksa A, Artavanis-Tsakonas S, Hariharan IK (2004). The *Drosophila* F box protein archipelago regulates dMyc protein levels in vivo. Curr Biol 14, 965–974.

Mongay L, Plaza S, Vigorito E, Serra-Pages C, Vives J (2001). Association of the cell cycle regulatory proteins p45(SKP2) and CksHs1. Functional effect on CDK2 complex formation and kinase activity. J Biol Chem 276, 25030–25036.

Morgan DO (1995). Principles of CDK regulation. Nature 374, 131–134.

Morisaki H, Fujimoto A, Ando A, Nagata Y, Ikeda K, Nakanishi M (1997). Cell cycle-dependent phosphorylation of p27 cyclin-dependent kinase (Cdk) inhibitor by cyclin E/Cdk2. Biochem Biophys Res Commun 240, 386–390.

Nakayama K, Nagahama H, Minamishima YA, Miyake S, Ishida N, Hatakeyama S, Kitagawa M, Iemura S, Natsume T, Nakayama KI (2004). Skp2-mediated degradation of p27 regulates progression into mitosis. Dev Cell 6, 661–672.

Neufeld TP, de la Cruz AF, Johnston LA, Edgar BA (1998). Coordination of growth and cell division in the *Drosophila* wing. Cell 93, 1183–1193.

Otsu N (1979). A threshold selection method from gray-level histograms. IEEE Trans Syst Man Cybern 9, 62–66.

Pagano M (2004). Control of DNA synthesis and mitosis by the Skp2-p27-Cdk1/2 axis. Mol Cell 14, 414–416.

Pateras IS et al. (2006). Downregulation of the KIP family members p27(KIP1) and p57(KIP2) by SKP2 and the role of methylation in p57(KIP2) inactivation in nonsmall cell lung cancer. Int J Cancer 119, 2546–2556.

Sauer K, Knoblich JA, Richardson H, Lehner CF (1995). Distinct modes of cyclin E/cdc2c kinase regulation and S-phase control in mitotic and endoreduplication cycles of *Drosophila* embryogenesis. Genes Dev 9, 1327–1339.

Signoretti S, Di Marcotullio L, Richardson A, Ramaswamy S, Isaac B, Rue M, Monti F, Loda M, Pagano M (2002). Oncogenic role of the ubiquitin ligase subunit Skp2 in human breast cancer. J Clin Invest 110, 633–641.

Skaar JR, D'Angiolella V, Pagan JK, Pagano M (2009a). SnapShot: F box proteins II. Cell 137, 1358, 1358e1.

Skaar JR, Pagan JK, Pagano M (2009b). SnapShot: F box proteins I. Cell 137, 1160–1160e1.

Spruck C, Strohmaier H, Watson M, Smith AP, Ryan A, Krek TW, Reed SI (2001). A CDK-independent function of mammalian Cks1: targeting of SCF(Skp2) to the CDK inhibitor p27Kip1. Mol Cell 7, 639–650.

Swan A, Schupbach T (2007). The Cdc20 (Fzy)/Cdh1-related protein, Cort, cooperates with Fzy in cyclin destruction and anaphase progression in meiosis I and II in *Drosophila*. Development 134, 891–899.

Tedesco D, Lukas J, Reed SI (2002). The pRb-related protein p130 is regulated by phosphorylation-dependent proteolysis via the protein-ubiquitin ligase SCF(Skp2). Genes Dev 16, 2946–2957.

Thomer M, May NR, Aggarwal BD, Kwok G, Calvi BR (2004). *Drosophila* double-parked is sufficient to induce re-replication during development and is regulated by cyclin E/CDK2. Development 131, 4807–4818.

Tsvetkov LM, Yeh KH, Lee SJ, Sun H, Zhang H (1999). p27(Kip1) ubiquitination and degradation is regulated by the SCF(Skp2) complex through phosphorylated Thr187 in p27. Curr Biol 9, 661–664.

Vermeulen K, Van Bockstaele DR, Berneman ZN (2003). The cell cycle: a review of regulation, deregulation and therapeutic targets in cancer. Cell Prolif 36, 131–149.

von der Lehr N et al. (2003). The F-box protein Skp2 participates in c-Myc proteosomal degradation and acts as a cofactor for c-Myc-regulated transcription. Mol Cell 11, 1189–1200.

Wang W, Ungermannova D, Chen L, Liu X (2003). A negatively charged amino acid in Skp2 is required for Skp2-Cks1 interaction and ubiquitination of p27Kip1. J Biol Chem 278, 32390–32396.

Wang W, Ungermannova D, Chen L, Liu X (2004). Molecular and biochemical characterization of the Skp2-Cks1 binding interface. J Biol Chem 279, 51362–51369.

Wang XC, Tian LL, Tian J, Jiang XY (2012). Overexpression of SKP2 promotes the radiation resistance of esophageal squamous cell carcinoma. Radiat Res 177, 52–58.

Wang Z, Gao D, Fukushima H, Inuzuka H, Liu P, Wan L, Sarkar FH, Wei W (2012). Skp2: A novel potential therapeutic target for prostate cancer. Biochim Biophys Acta 1825, 11–17.

Wei B, Chen Z, Zhang X, Feldman M, Dong XZ, Doran R, Zhao BL, Yin WX, Kotlikoff MI, Ji G (2008). Nitric oxide mediates stretch-induced Ca2+ release via activation of phosphatidylinositol 3-kinase-Akt pathway in smooth muscle. PLoS One 3, e2526.

Wei B, Gao J, Huang XP, Jin JP (2010). Mutual rescues between two dominant negative mutations in cardiac troponin I and cardiac troponin T. J Biol Chem 285, 27806–27816.

Weigmann K, Cohen SM, Lehner CF (1997). Cell cycle progression, growth and patterning in imaginal discs despite inhibition of cell division after inactivation of Drosophila Cdc2 kinase. Development 124, 3555–3563.

Whittaker AJ, Royzman I, Orr-Weaver TL (2000). Drosophila double parked: a conserved, essential replication protein that colocalizes with the origin recognition complex and links DNA replication with mitosis and the down-regulation of S phase transcripts. Genes Dev 14, 1765–1776.

Wojda I (2000). The group of protein kinases CKI [in Polish]. Postepy Biochem 46, 140–147.

Xie G, Zhang H, Du G, Huang Q, Liang X, Ma J, Jiao R (2012). Uif, a large transmembrane protein with EGF-like repeats, can antagonize Notch signaling in Drosophila. PLoS One 7, e36362.

Xu Y, Lei Z, Huang H, Dui W, Liang X, Ma J, Jiao R (2009). dRecQ4 is required for DNA synthesis and essential for cell proliferation in Drosophila. PLoS One 4, e6107.

Yam CH, Ng RW, Siu WY, Lau AW, Poon RY (1999). Regulation of cyclin A-Cdk2 by SCF component Skp1 and F-box protein Skp2. Mol Cell Biol 19, 635–645.

Yao ZP, Zhou M, Kelly SE, Seeliger MA, Robinson CV, Itzhaki LS (2006). Activation of ubiquitin ligase SCF(Skp2) by Cks1: insights from hydrogen exchange mass spectrometry. J Mol Biol 363, 673–686.

Yeh KH, Kondo T, Zheng J, Tsvetkov LM, Blair J, Zhang H (2001). The F-box protein SKP2 binds to the phosphorylated threonine 380 in cyclin E and regulates ubiquitin-dependent degradation of cyclin E. Biochem Biophys Res Commun 281, 884–890.

Yu ZK, Gervais JL, Zhang H (1998). Human CUL-1 associates with the SKP1/SKP2 complex and regulates p21(CIP1/WAF1) and cyclin D proteins. Proc Natl Acad Sci USA 95, 11324–11329.

Yung Y, Walker JL, Roberts JM, Assoian RK (2007). A Skp2 autoinduction loop and restriction point control. J Cell Biol 178, 741–747.

Zhu L (2010). Skp2 knockout reduces cell proliferation and mouse body size: and prevents cancer? Cell Res 20, 605–607.

Zielke N et al. (2011). Control of Drosophila endocycles by E2F and CRL4(CDT2). Nature 480, 123–127.